minerals

MDPI

Article

Potential for CO_2 Mineral Carbonation in the Paleogene Segamat Basalt of Malaysia

Syifa Afiza Ayub [1], Haylay Tsegab [1,2,*], Omeid Rahmani [3] and Amin Beiranvand Pour [4,*]

1 Department of Geosciences, Universiti Teknologi PETRONAS (UTP), Perak 32610, Malaysia; syifa_17008712@utp.edu.my
2 Southeast Asia Carbonate Research Laboratory, Universiti Teknologi PETRONAS (UTP), Perak 32610, Malaysia
3 Department of Natural Resources Engineering and Management, School of Science and Engineering, University of Kurdistan Hewlêr (UKH), Erbil 44001, Kurdistan Region, Iraq; omeid.rahmani@ukh.edu.krd
4 Institute of Oceanography and Environment (INOS), Universiti Malaysia Terengganu (UMT), Kuala Nerus 21030, Terengganu, Malaysia
* Correspondence: haylay.tsegab@utp.edu.my (H.T.); beiranvand.pour@umt.edu.my (A.B.P.); Tel.: +86-60-5-368-7347 (H.T.); +60-9-668-3824 (A.B.P.)

Received: 26 October 2020; Accepted: 22 November 2020; Published: 24 November 2020

Abstract: Geological storage of carbon dioxide (CO_2) requires the host rock to have the capacity to permanently store CO_2 with minimum post-storage monitoring. Mineral carbonation in geological formations is one of the most promising approaches to CO_2 storage as the captured CO_2 is converted into stable carbonated minerals (e.g., calcite and magnesite). In this study, we investigated the geochemical and mineralogical characteristics of Segamat basalt in the Central Belt of Malaysia and evaluated its potential for mineral carbonation by using laboratory analyses of X–ray fluorescence (XRF), X–ray diffraction analysis (XRD) and petrographic study. The XRF results showed that Segamat basalt samples contain a number of elements such as Fe (21.81–23.80 wt.%), Ca (15.40–20.83 wt.%), and Mg (3.43–5.36 wt.%) that can react with CO_2 to form stable carbonated minerals. The XRD and petrographic results indicated that Segamat basalt contains the reactive mineral groups of pyroxene and olivine, which are suitable for the mineral carbonation process. The results of this study could help to identify the spatial distribution of elements and minerals in the Segamat basalt and to assess its mineral carbonation potential for geological storage in Malaysia.

Keywords: CO_2 sequestration; mineral carbonation; geological storage; Segamat basalt; Malaysia

1. Introduction

The atmospheric concentration of carbon dioxide (CO_2), as well as other greenhouse gases (GHGs), has become a central issue for researchers due to its significant effect on global warming [1–4]. The objective of a carbon capture storage (CCS) approach is to help decrease the amount of carbon dioxide (CO_2) that is emitted globally from industrial areas through the capture of the produced CO_2. CCS is considered to be one of the safest ways of achieving this, and storing CO_2 in geological formations, such as in depleted oil and gas reservoirs is one of the proposed solutions in CCS strategies [1,5,6]. These reservoirs used to contain hydrocarbon at high pressure for a certain geological period, which proves that they have the potential to be used for the storage of CO_2 [7]. However, there are some challenges associated with the CCS technique. The most critical issue is the possibility of CO_2 leakage. Understanding the geochemical characterization of the geological formation is crucial to ensure the permanency of the CO_2 storage in the mineral interaction of the host rock with the injected CO_2 [8,9].

Mineral carbonation has been proposed as an alternative mechanism to mitigate the CO_2 concentration in the Earth's atmosphere through its sequestration as stable carbonate minerals [10–14]. Mineral carbonation is commonly associated with common elements such as calcium (Ca), magnesium (Mg), and iron (Fe) contained in natural minerals and rocks because their characteristics allow them to react to CO_2 and to form carbonated products [15]. It is a process whereby CO_2 is chemically reacted with Ca-, Mg-, or Fe-containing minerals to form carbonated minerals, which do not require any long-term liability or monitoring commitments [10,16]. Additionally, the mineral carbonation process can be applied to reuse various products, which positively influences the environmental impact and reduces the process cost [2,4,17,18].

Basalts are rich in Ca, Mg, and Fe cations that are readily liberated by reaction with CO_2–rich water [19]. Therefore, in situ mineral carbonation is likely to be more active in basalts [19–21]. Silicate minerals (i.e., olivine and pyroxene) and glasses are rapidly dissolved in the accelerated in situ mineral carbonation of basalts [22,23]. This process leads to the release of divalent cations, which tend to react with CO_2 in precipitating the carbonated minerals rather than forming other secondary minerals such as clays, oxides, and zeolites [22]. To date, there has been little discussion regarding the geochemical and mineralogical characterization of basalts for assessing their potential in the process of CO_2 sequestration by mineral carbonation [22,24]. In this study, samples from a Tertiary extrusive igneous body, Segamat basalt were characterized to evaluate its geochemical and mineralogical properties and to estimate its potential as a host rock for CO_2 storage through the in situ mineral carbonation process. Besides, Segamat basalt could be used as a source for the ex situ mineral carbonation process in the Malay Peninsula by determining whether Segamat basalt contains the required ingredients, i.e., the presence of Ca, Mg, or Fe-bearing minerals for the CO_2 mineral carbonation process to occur or not.

2. Geological Setting

The Malay Peninsula forms an integral part of the SE Asian continental core of Sundaland [25,26]. It comprises two tectonic blocks: the Sibumasu Terrane in the west and the Sukhothai Arc in the east of the Malaya Block [27]. As shown in Figure 1, the Malay Peninsula is characterized by three north–south trending longitudinal belts, including the Western Belt, Central Belt, and Eastern Belt [27,28].

Flows of alkaline basaltic lava has occurred twice in the Malay Peninsula. These have been reported around Kuantan and in the neighborhood of Pekan Jabi in Segamat [29–31]. These volcanic rocks are named after the localities as Kuantan basalt and Segamat basalt. The Segamat volcanism includes both lava and shallow intrusive rocks (Figure 1), and individual lava flows vary from 18 m to 42 m in thickness [29,31]. Segamat basalt was formed as post-orogenic flows within the Central Belt of the Malay Peninsula during the Cenozoic Era (Figure 1). It erupted in the Early Tertiary period and has been dated as Palaeocene (62 ± 3 Ma) by K–Ar dating [32], during a time in which the Malay Peninsula was considered as a tectonically stable block [33]. The main area of Segamat basalt outcrops is located in the State of Johor, Malaysia (Figure 1).

Field Occurrence of Segamat Basalt

Segamat basalt presents as dark green to black colored outcrops (Figure 2a) and in the field, it is mainly characterized by its fine-grained porphyritic texture. Segamat basalt contains very fine groundmass with visible phenocrysts of light-green colored minerals (Figure 2b). Olivine and pyroxene occur as the greenish phenocrysts in the groundmass rock specimen. These greenish phenocrysts have undergone a relatively slow rate of cooling at the near surface before reaching the surface. The early-formed phenocrysts represent basic-ultrabasic olivine/pyroxene minerals. The dominant fine groundmass indicates that there was a second phase of relatively fast cooling during the extrusion of the magma to the surface and the atmosphere.

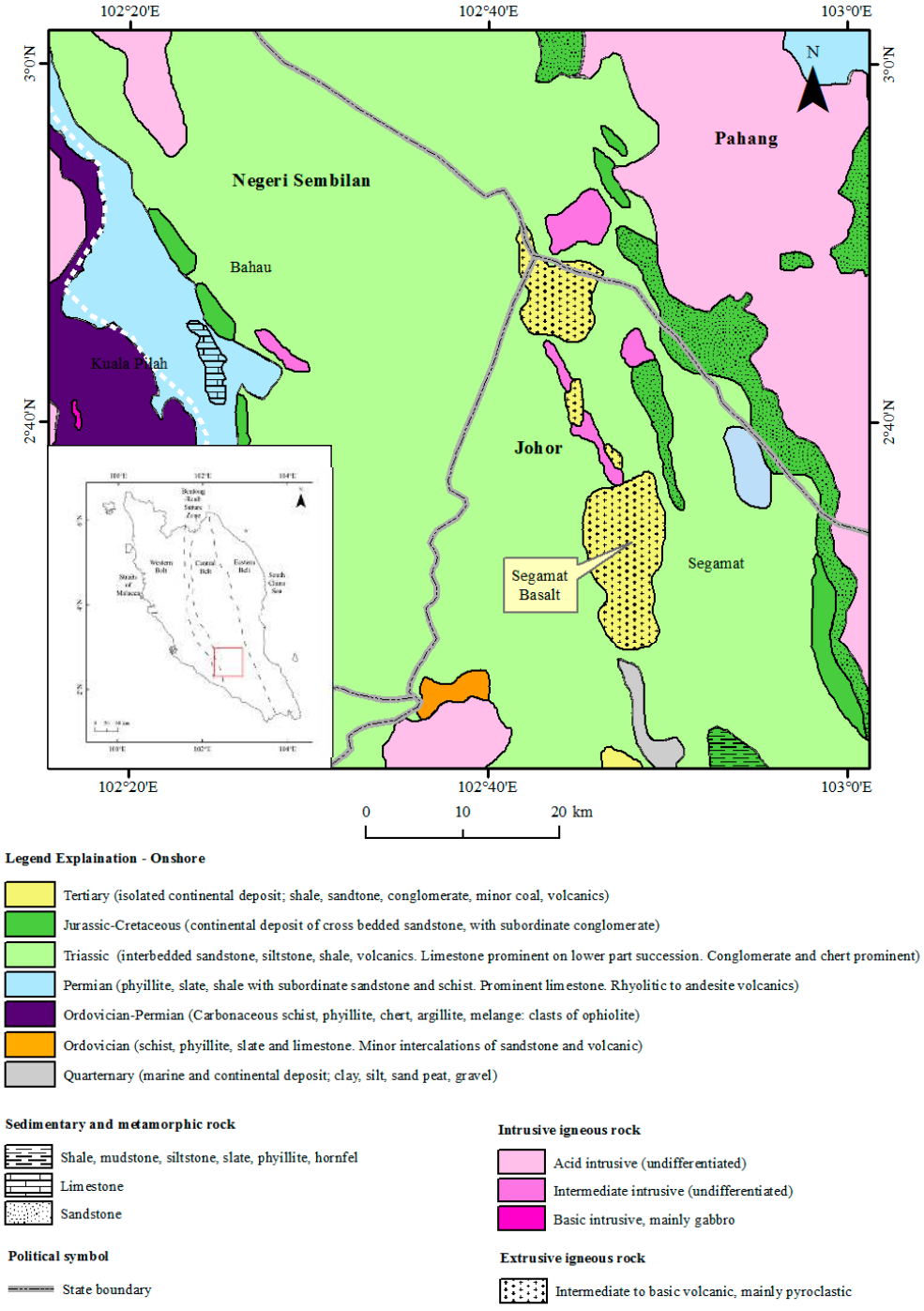

Figure 1. Geological map of Segamat basalt modified from Ng et al. [34].

As shown in Figure 2a, the presence of calcite veins has been documented in the Segamat basalt outcrops. The calcite veins have sharp and straight edges with minimal irregularity on the contact surfaces with the host rock. The genesis of the calcite veins in Segamat basalt is associated with its hydrothermal origin [35].

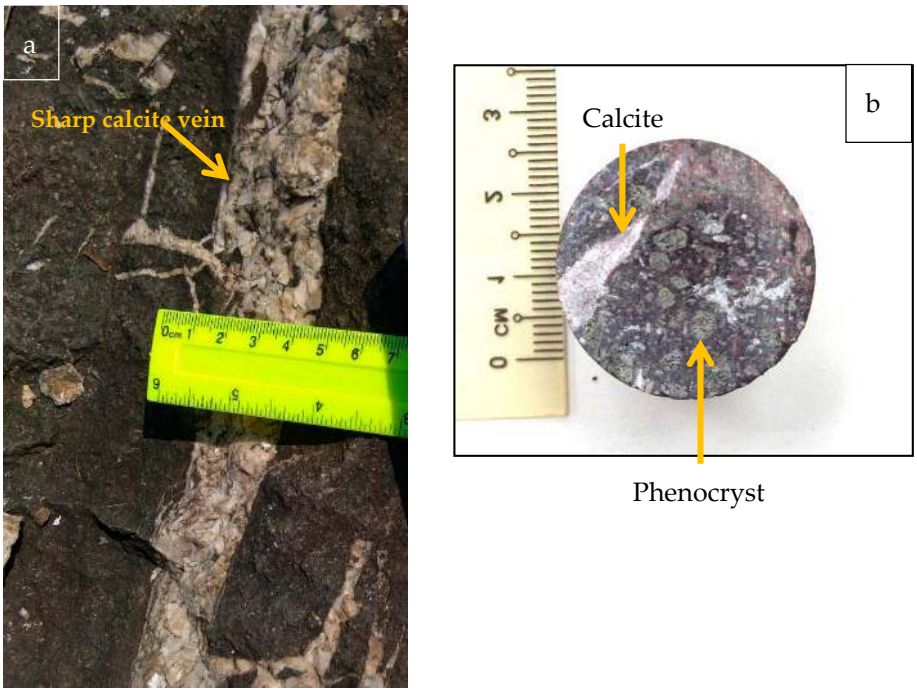

Figure 2. Calcite veins (**a**) and mafic phenocrysts (**b**) from the Segamat basalt outcrop.

3. Materials and Methods

Sample Preparation and Experimental Analysis

The following analyses were conducted to obtain an overview of the characteristics of the Segamat basalt samples. Sampling was carried out to characterize the host rock of the Segamat basalt with regard to its geochemical and mineralogical properties. Standardizing the grain size is essential in order to prevent biased results regarding the elements in these grain, and reducing the grain size enhances the precision of the analyses [36,37]. Therefore, the samples of Segamat basalt were crushed and prepared in a powder form with a grain size of <63 µm, which was determined by a MASTERSIZER–2000 from Malvern Instruments. The samples were studied by a microscope (Zeiss Axioskop–40, Oberkochen, Germany) to study the petrography of the Segamat basalt samples. To this aim, thin sections were prepared by slabbing and polishing the samples before they were glued onto the glass. Then, thin sections were examined under a plane-polarized light (PPL) and cross-polarized light (XPL) microscope (Zeiss Axioskop–40, Oberkochen, Germany), equipped with a Jenoptik ProgRes CF Scan microscope camera at the Southeast Asia Carbonate Research Laboratory, Universiti Teknologi PETRONAS. The PPL and XPL were used to identify the minerals and determine the textural components of the samples, respectively.

The powdered rock samples were analyzed to determine the major elemental composition of the Segamat basalt by using X–ray fluorescence (XRF) S8 TIGER Series 2 from Bruker HighSense Technology. The samples were ground to a grain size of <63 µm and were then combined with a cellulose wax mixture to produce homogeneous samples. Interaction between the atoms of the sample and radiation from the XRF instrument made the analysis of the chemical composition possible. Subsequently, the Segamat basalt sample was ionized by radiation of short wavelength and high-energy. A tightly-held inner electron was forced out when enough radiation was consumed. Then, an outer electron was replaced by an inner one. After that, the energy was released because the binding energy of the inner electron was decreased in comparison to the outer one. Moreover, because the amount of energy emitted was less than the initial incident X–rays, it is labeled as "fluorescent radiation". A transition between definite electron orbitals in a specific element was characterized by the energy of

the emitted photon, which suggested that XRF analysis could be applied to identify the concentration of the elements in the Segamat basalt sample.

X-ray diffraction (XRD) analysis was also applied to identify the mineral phases in the Segamat basalt samples. Thus, 1 g of each sample with a grain size of <63 µm was dried in an oven (at 45 °C) for 24 h and then introduced into the XRD instrument. The scan speed was set at 1°/min from 5° to 50° under 40 kV/40 mÅ X-ray tube. The XRD patterns were attained from a Rigaku Geiger flex D–MAX/A diffractometer with the Cu–Kα radiation along with a wavelength of 1.54 Å [4].

Field-emission scanning electron microscopy (FESEM, SU8030 Hitachi) was applied to assess the morphology of the grains and identify the surface roughness. The FESEM was linked with an energy-dispersive X-ray (EDX) spectroscopy to find the elemental composition of the sample at a specific surface location [38]. The FESEM analysis was performed at 2.2 nm (1 kV) and a 1 nm (15 kV) probe current. The Segamat basalt samples with a grain size of <63 µm were coated with gold and sputtered in the environment with an inert argon for the FESEM analysis. The samples were also qualitatively analyzed in terms of their chemical and crystalline phases by using the FESEM in combination with the EDX technology.

4. Results and Discussion

4.1. Geochemical Analysis

Tables 1 and 2 provide an overview of the significant elements found in the four samples of Segamat basalt by XRF analysis. As shown in Table 1, the Segamat basalt samples consist mainly of SiO_2 (41.78–44.58 wt.%), Fe_2O_3 (13.73–16.28 wt.%), CaO (11.20–15.74 wt.%), Al_2O_3 (11.70–13.10 wt.%), MgO (4.14–6.54 wt.%), and K_2O (4.21–5.59 wt.%). Table 2 presents the elemental analysis of the Segamat basalt samples. The Si content ranges between 30.05 and 33.30 wt.%. The samples contain Fe (21.81–23.80 wt.%), Ca (15.40–20.83 wt.%), Al (9.07–10.40 wt.%), K (1.11–2.06 wt.%), Mg (3.43–5.36 wt.%), and Ti (1.93–2.11 wt.%). As shown in the previous literature, the feedstock is rich in Ca, Mg, and Fe and is suitable for mineral carbonation process [4,7,11]. What is notable about these results is that Segamat basalt has a high percentage of reactants, and thus it has remarkable potential for the process of CO_2 mineral carbonation.

Table 1. Oxide composition of Segamat basalt from the XRF analysis.

Elements	Weight % in Sample 1	Weight % in Sample 2	Weight % in Sample 3	Weight % in Sample 4
SiO_2	43.90	41.78	44.58	41.95
Fe_2O_3	13.73	16.28	14.86	16.07
$Al2O_3$	13.10	11.70	12.60	12.30
CaO	11.20	13.71	14.19	15.74
MgO	6.54	5.46	4.14	4.80
K_2O	5.23	5.95	4.30	4.21
P_2O_5	2.85	1.47	1.37	1.52
TiO_2	1.43	1.69	1.75	1.60
Na_2O	0.62	0.92	1.30	0.90
MnO	0.28	0.35	0.29	0.31
SO_3	0.24	–	0.07	0.06
BaO	0.24	0.33	0.17	0.19
Cl	0.20	0.08	0.07	0.07
CuO	0.16	0.04	0.04	0.04
ZnO	0.10	0.05	0.05	0.05
Cr_2O_3	0.06	0.07	0.06	0.05
SrO	0.06	0.08	0.08	0.10
ZrO_2	–	0.03	0.09	0.02
Rb_2O	0.03	0.03	0.02	0.02
NiO	–	0.02	0.02	0.02

Table 2. Elemental composition of Segamat basalt from the XRF analysis.

Elements	Weight % in Sample 1	Weight % in Sample 2	Weight % in Sample 3	Weight % in Sample 4
Si	33.30	30.32	32.88	30.05
Fe	21.81	23.49	22.40	23.80
Ca	15.40	18.19	19.10	20.83
Al	10.40	9.07	9.59	9.57
K	8.11	8.68	6.48	6.27
Mg	5.36	4.55	3.43	3.97
P	2.06	1.12	1.11	1.11
Ti	1.83	2.00	2.11	1.93
Na	–	0.64	1.40	0.79
Mn	0.46	0.52	0.50	0.47
Ba	0.36	0.63	0.16	0.36
Cu	0.31	0.06	0.07	0.08
Zn	0.20	0.10	0.09	0.10
Sr	0.14	0.15	0.16	0.20
Cr	0.11	0.09	–	0.08
Rb	0.06	0.07	0.05	0.05
Ni	0.05	0.04	0.04	0.03
Zr	–	0.16	0.15	0.14
Cl	–	0.11	0.13	0.15

4.2. Mineralogical Analysis

Figure 3 presents a comparison between the PPL and XPL studies of the Segamat basalt samples. Carbonate and feldspar minerals were identified as phenocrysts as shown in Figure 3a,b. Figure 3c,d also depict carbonate and olivine minerals as phenocrysts. Figure 3e,f show the presence of orthopyroxene as a large phenocryst. Other phenocrysts include olivine, chlorite, and carbonate with a wide distribution of feldspar. Figure 3g,f show that the minerals of olivine, orthopyroxene, and feldspar appear as phenocrysts. Figure 3 shows that the texture of Segamat basalt is porphyritic, it contains fine groundmass and shows phenocrysts as the minerals identified above. The porphyritic texture that is shown under microscope is similar to that observed in the sample shown in Figure 2b. The average porosity of the samples is 16%, based on the study of more than 75 thin sections of the Segamat basalt.

Figures 4–7 present the mineralogical identification of Segamat basalt samples using XRD spectrum peaks. In accordance with previously reported data [24], the main crystalline phase of Segamat basalt is an olivine group including fayalite (Fe_2SiO_4) at the 2θ position of 31.6° and 35.9°, and forsterite (Mg_2SiO_4) at the 2θ position of 32.0°, 35.4° and 36.4°. Other crystalline phases are the pyroxene, chlorite, alkali feldspar, plagioclase, and zeolite group. The pyroxene group includes enstatite ($Mg_2Si_2O_6$) and augite ($(Ca,Na)(Mg,Fe,Al,Ti)(Si,Al)_2O_6$), which mainly occur at the 2θ position of 28.3° and 35.6°, respectively. From the chlorite group, sudoite ($Mg_2Al_3(Si_3Al)O_{10})(OH)_8$) appears at the 2θ position of 6.2°, 19.6°, 12.4°, 25.2°, and 44.8°. The peaks of 20.9°, 24.1°, 27.4°, and 30.7° refer to microcline ($KAlSi_3O_8$) while 21.09°, 23.6° and 27.0° donate orthoclase ($KAlSi_3O_8$). Both microcline and orthoclase are categorized as alkali feldspars. Also, the plagioclase group presents as anorthite ($Ca(Al_2Si_2O_8)$) at the 2θ position of 22.0°, 23.7°, 28.1°, and 30.6°. The peaks of 15.78° and 25.97° donate analcime ($Na(AlSi_2O_6)\cdot H_2O$) as the zeolite group. A shown in Tables 1 and 2, the XRF results strongly support the mineralogical identification of oxides and elements that are considered to have potential in the process of CO_2 mineral carbonation.

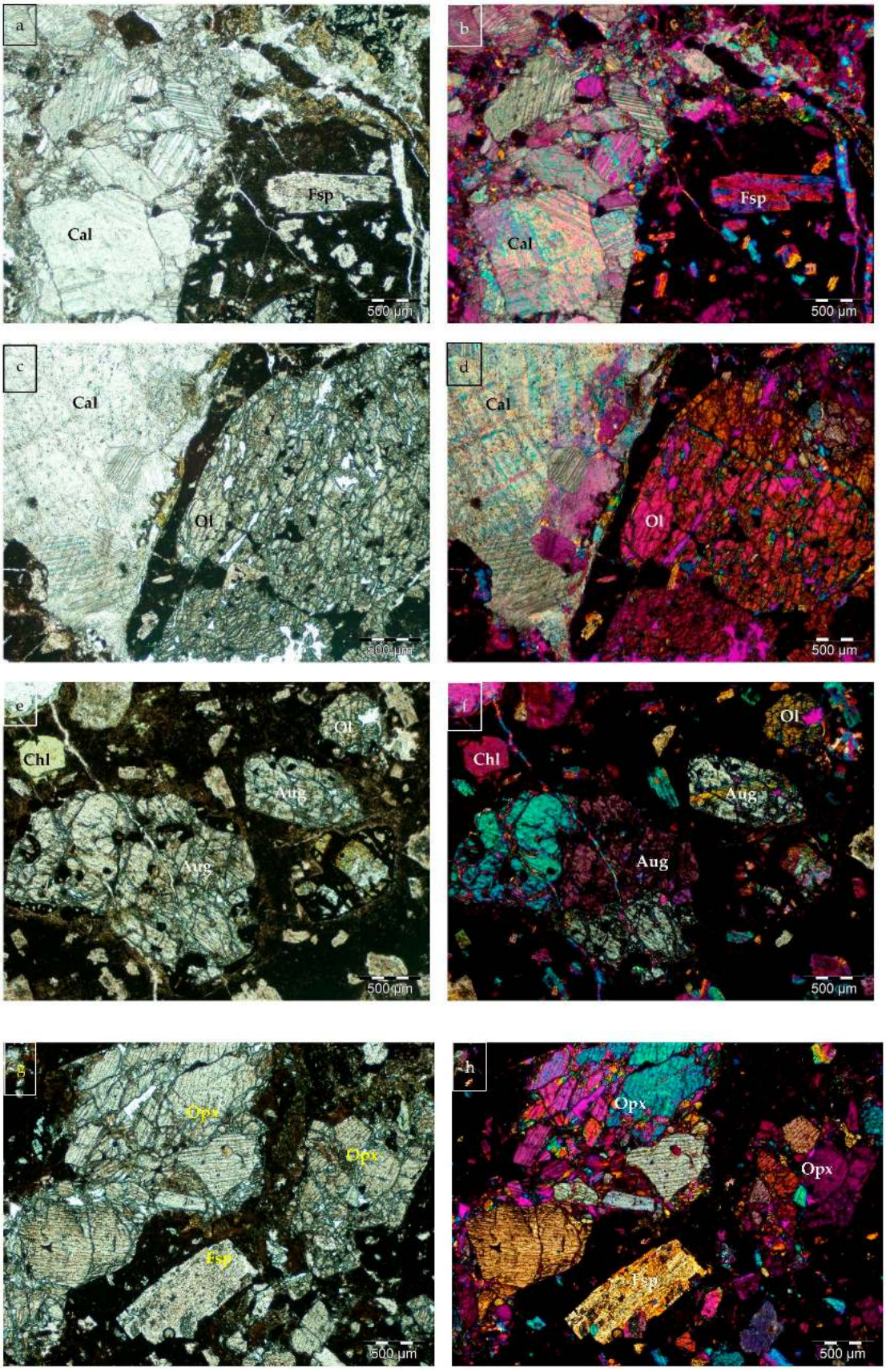

Figure 3. Petrography of Segamat basalt samples under PPL (**a**,**c**,**e**,**g**) and XPL (**b**,**d**,**f**,**h**) using 4× magnification. Cal, Fsp, Ol, Chl, Aug, and Opx represent calcite, feldspar, olivine, chlorite, augite, and orthopyroxene, respectively.

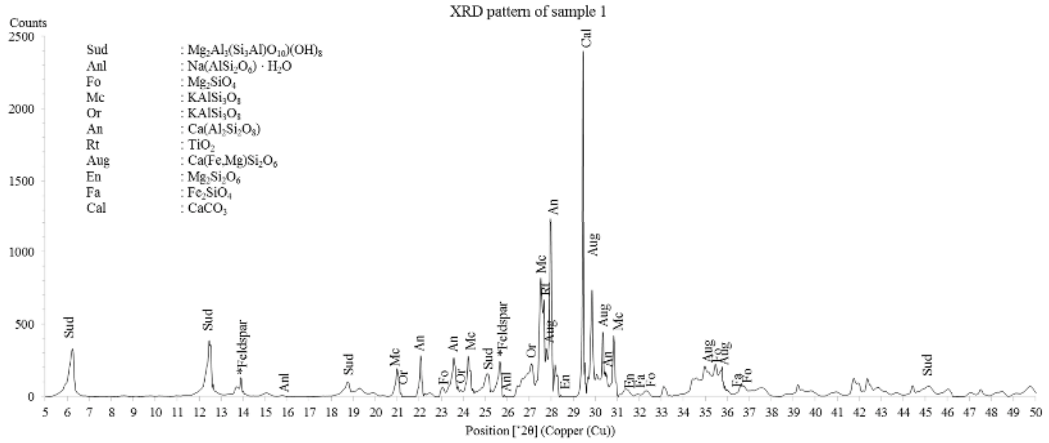

Figure 4. XRD analysis of sample 1 from Segamat basalt (Chl:chlorite, Sud: sudoite, *Feldspar: common feldspar group peak, Anl: analcime, Afs: alkali feldspar, Mc: microcline, An: anorthite, Fo: forsterite, Or: orthoclase, Rt: rutile, Aug: augite, Hyp: hypersthene, Cal: calcite, En: enstatite, Fa: fayalite).

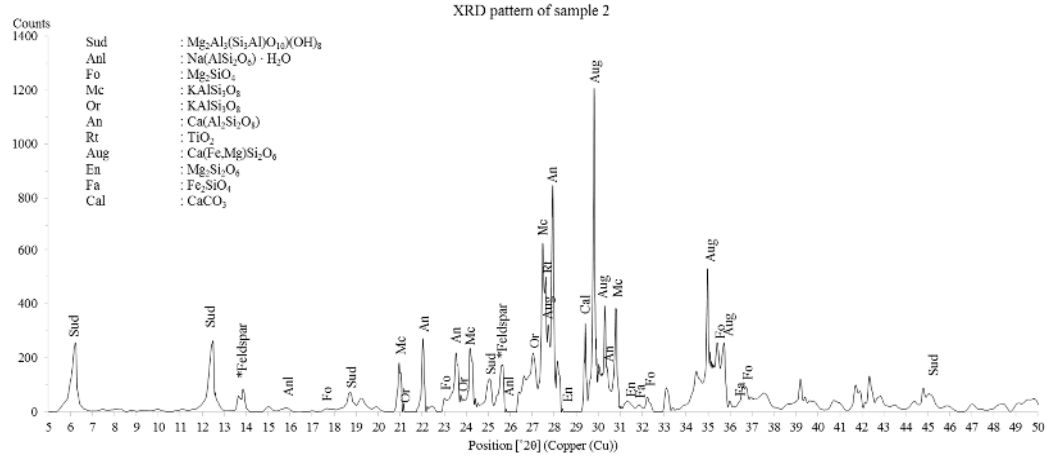

Figure 5. XRD analysis sample 2 of the Segamat basalt (Chl: chlorite, Sud: sudoite, *Feldspar: common feldspar group peak, Anl: analcime, Afs: alkali feldspar, Mc: microcline, An: anorthite, Fo: forsterite, Or: orthoclase, Rt: rutile, Aug: augite, Hyp: hypersthene, Cal: calcite, En: enstatite, Fa: fayalite).

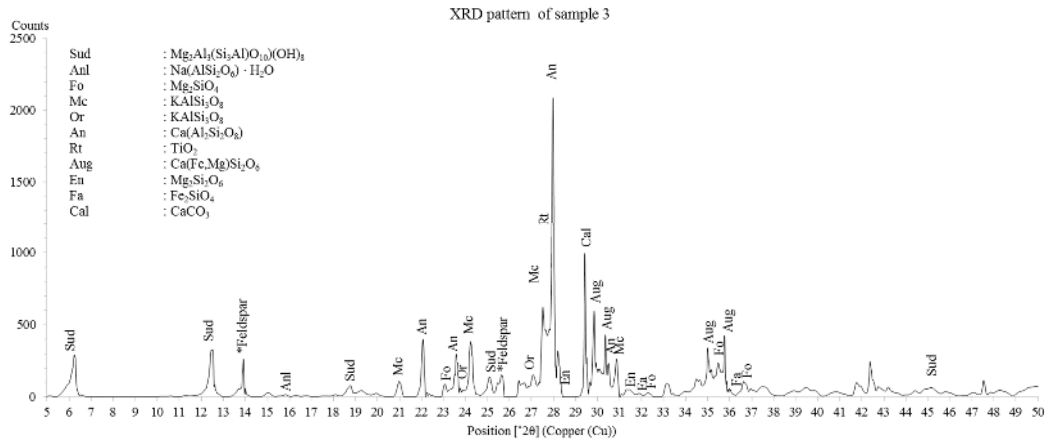

Figure 6. XRD analysis of sample 3 of the Segamat Basalt (Chl: chlorite, Sud: sudoite, *Feldspar: common feldspar group peak, Anl: analcime, Afs: alkali feldspar, Mc: microcline, An: anorthite, Fo: forsterite, Or: orthoclase, Rt: rutile, Aug: augite, Hyp: hypersthene, Cal: calcite, En: enstatite, Fa: fayalite).

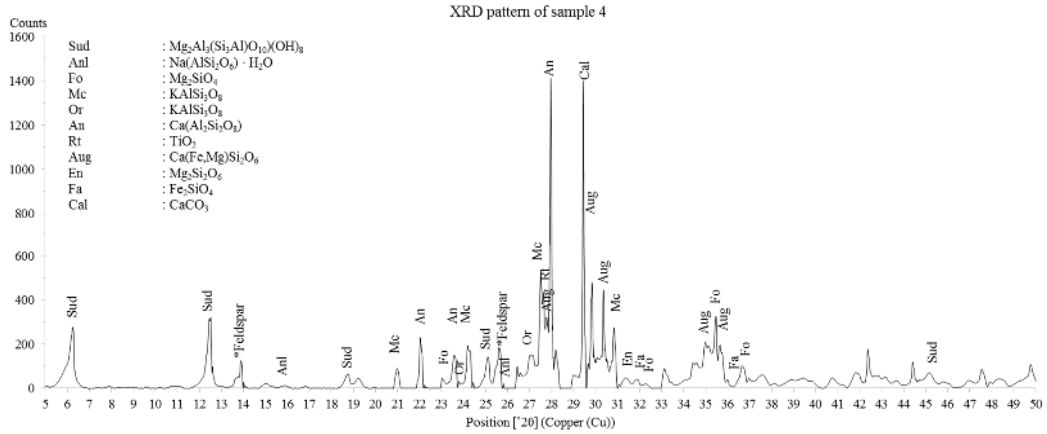

Figure 7. XRD analysis of sample 4 of the Segamat basalt (Chl: chlorite, Sud: sudoite, *Feldspar: common feldspar group peak, Anl: analcime, Afs: alkali feldspar, Mc: microcline, An: anorthite, Fo: forsterite, Or=: orthoclase, Rt: rutile, Aug: augite, Hyp: hypersthene, Cal: calcite, En: enstatite, Fa: fayalite).

The XRD results from the thin sections were consistent with the XPL results, which clearly showed the texture of the Segamat basalt including orthopyroxene, olivine, and augite (see Figure 3). Aside from that, other phenocrysts such as calcite, feldspar, and chlorite minerals were identified in the thin sections, and this was also supported by the XRD analysis (see Figures 4–7).

4.3. Segamat Basalt Potential for CO_2 Mineral Carbonation

To determine whether the selected samples are suitable for the process of mineral carbonation, it is essential to understand their geochemical and mineralogical characteristics. Several reports have shown that only a few basaltic types are suitable to serve as host rocks in the CO_2 mineral carbonation process [21,39,40]. The results of this study indicated that the Segamat basalt samples have the proper geochemical and mineralogical properties for applying the CO_2 mineral carbonation process. These properties involve an appropriate content of Fe-, Mg-, and Ca-bearing minerals. The EDX spectrum (Figure 8) shows that the Segamat basalt samples are mainly composed of C, O, Na, Mg, Al, Si, K, Ca, Ti and Fe. Also, Figure 9 indicates that Ca, C, and O were the main elements detected by the EDX analysis. Additionally, the FESEM images show micro-pores ranging from 0.1–1.5 μm in diameter (Figure 9).

Based on the XRF results (see Table 2), Segamat basalt, as an ultramafic rock, is very suitable for the process of mineral carbonation because it contains a considerable amount of oxides such as CaO (11.20–15.74 wt.%) and MgO (4.14–6.54 wt.%) that can potentially be carbonated. These oxides are favored by divalent reactants to form another carbonate mineral (i.e., calcite and magnesite). Equations (1) and (2) show the reactions of these oxides with CO_2. The products of these two potential reactants would be calcite ($CaCO_3$) and magnesite ($MgCO_3$).

$$CaO + CO_2 \rightarrow CaCO_3 \quad (1)$$

$$MgO + CO_2 \rightarrow MgCO_3 \quad (2)$$

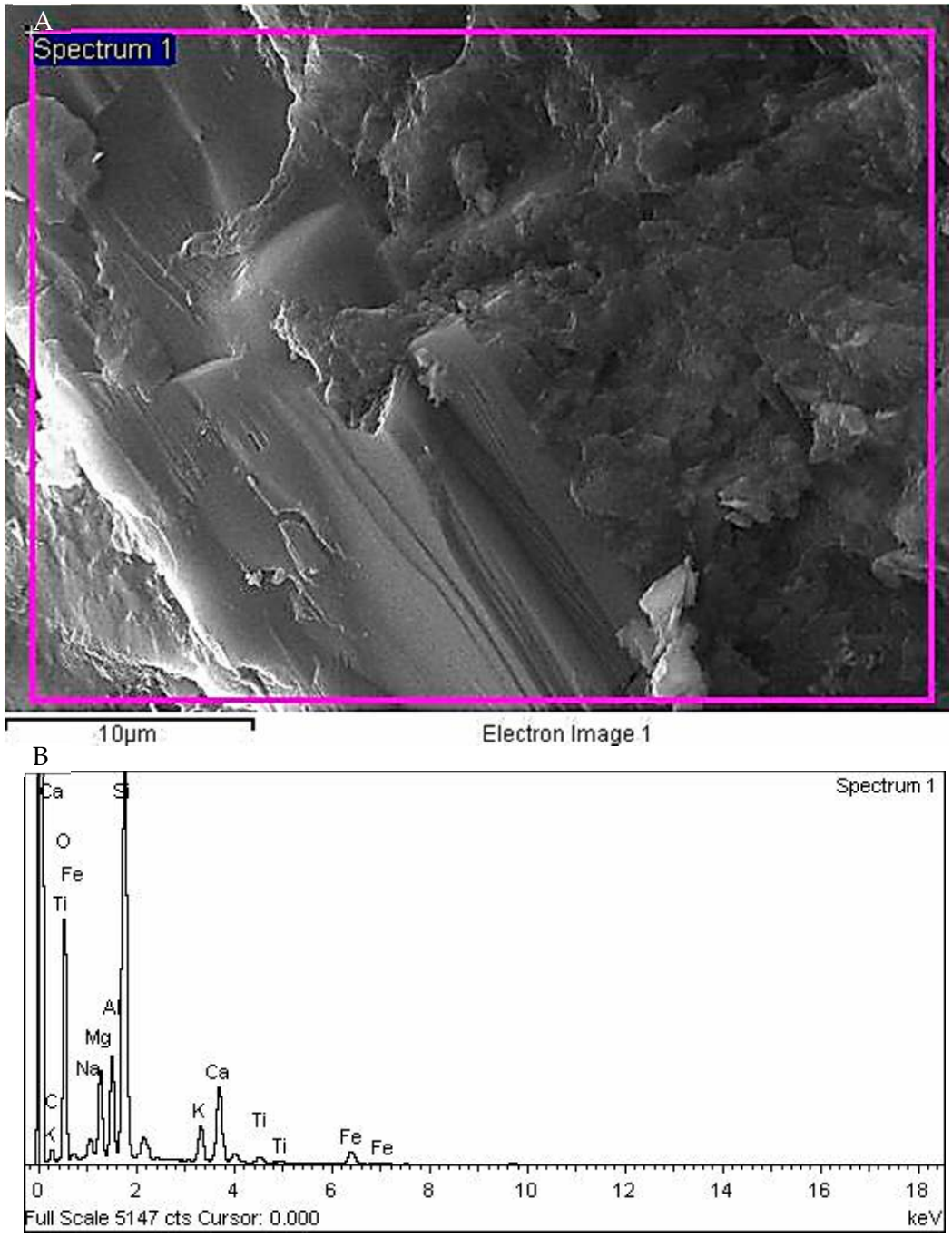

Figure 8. (**A**) FESEM image and (**B**) EDX spectrum of Segamat basalt sample. Element weight percentage (wt.%): C (0.91 wt.%), O (53.45 wt.%), Na (1.44 wt.%), Mg (4.76 wt.%), Al (5.01 wt.%), Si (22.11 wt.%), K (2.62 wt.%), Ca (6.25 wt.%), Ti (0.71 wt.%), and Fe (2.74 wt.%).

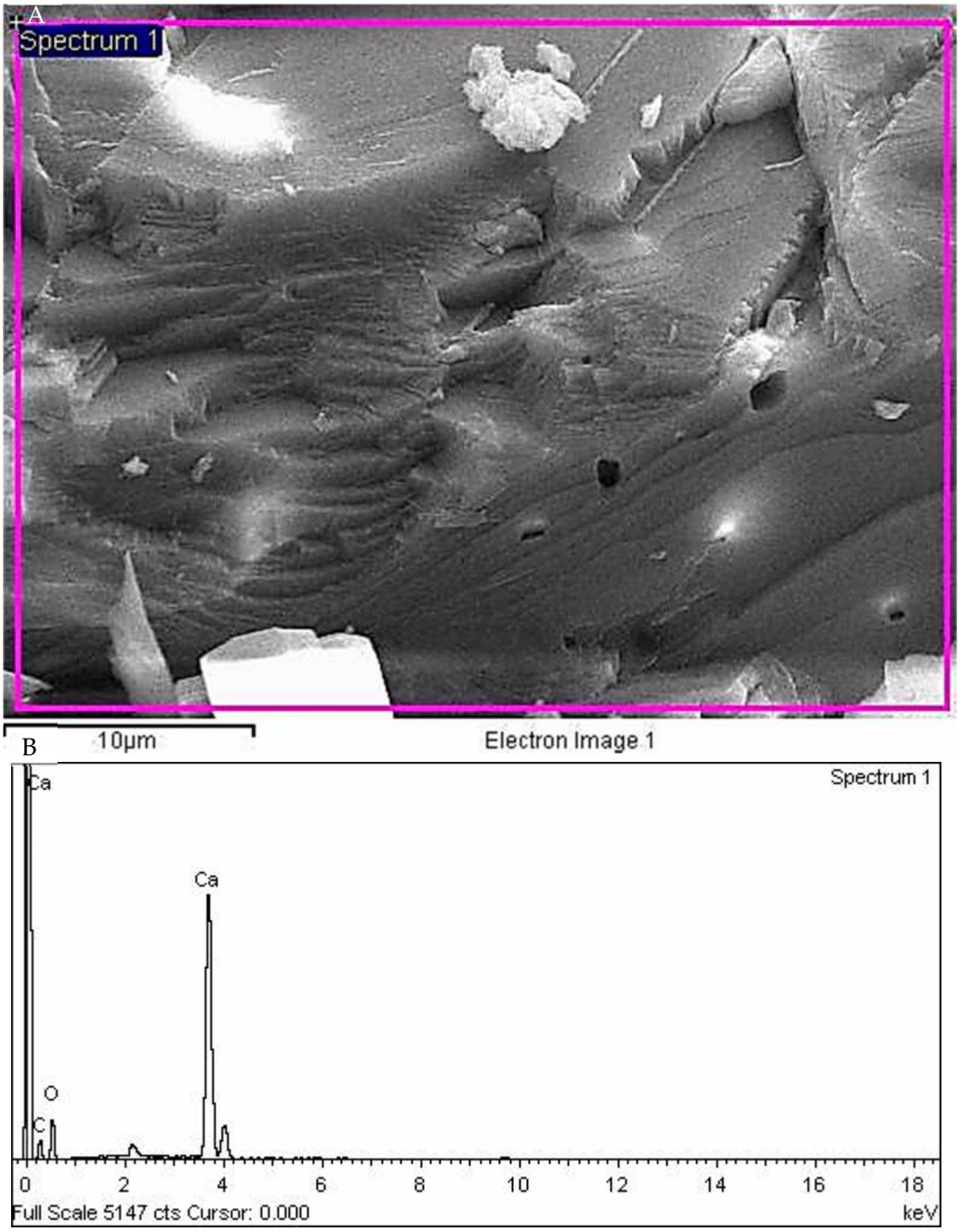

Figure 9. (**A**) FESEM image and (**B**) EDX spectrum of Segamat basalt sample. Elemental analysis by the EDX shows that C (7.99 wt.%), O (45.51 wt.%), and Ca (46.50 wt.%) are the main elements.

Moreover, mineral carbonation requires the dissolution of reactive minerals during CO_2–rich water interaction with the feedstock. It has been reported that the presence of water can increase the amount of carbonated minerals during the interaction of basalt samples with the injected CO_2 [41]. In this regard, the XRD analysis (see Figures 4–7) provides more precise results for identifying the minerals in the samples. It shows that Segamat basalt contains the pyroxene group (enstatite ($MgSiO_3$) and augite ($(Ca,Na)(Mg,Fe,Al)(Si,Al)_2O_6$)), and the olivine group (fayalite (Fe_2SiO_4) and forsterite (Mg_2SiO_4)), which enhance the mineral carbonation process in the feedstock (see Figure 4). At first, carbon dioxide is dissolved in water causing it to become acidic. When these reactive minerals react with the carbonated water, the dissolution process occurs and the cations of Ca, Mg, and Fe are released into the water. Later, these leached out cations precipitate into stable carbonated minerals like calcite

($CaCO_3$), magnesite ($MgCO_3$), and siderite ($FeCO_3$) when combined with the dissociated carbonic acid (Equations (3) and (4)).

$$CO_2 + H_2O \rightarrow H_2CO_3 \quad (3)$$

$$(Ca, Mg, Fe)^{2+} + H_2CO_3 \rightarrow (Ca, Mg, Fe)CO_3 + 2H^+ \quad (4)$$

As discussed above, the identification of pyroxene and olivine minerals in Segamat basalt is crucial because these minerals are the prerequisite for further reaction with CO_2 and water, which allows the process of mineral carbonation to occur [19]. Forsterite (Mg_2SiO_4) and anorthite ($Ca(Al_2Si_2O_8)$) minerals in basalts act as the potential source minerals for CO_2 sequestration. According to Oelkers et al. [19], 5.86 tons of forsterite and 23.1 tons of anorthite are required to sequester 1 ton of carbon dioxide. This means that olivine and pyroxene are more reactive than plagioclases for the process of mineral carbonation. Also, the existence of carbonated minerals such as calcite in the Segamat basalt proves that this feedstock has a natural potential for the process of mineral carbonation during geological time. There is no record in previous studies of the presence of calcite as phenocrysts in Segamat basalt.

Furthermore, the outcrops of Segamat basalt present a potential site for sequestering carbon dioxide. The Segamat basalts are located in Johor Province, Malaysia, with a strong source of CO_2 emissions in this area. The CCS approaches are applicable through the H_2O–CO_2 interaction to sequestrate CO_2 in the Segamat basalt. As can be seen in the FESEM images (see Figures 8 and 9), the CO_2 mineral carbonation process is increased since pore-space is highly available in the Segamat basalt samples. On the other hand, the Segamat basalts have been formed in the Paleogene period and are relatively less-altered by volcanic exposure, thus they are more feasible in the process of CO_2 mineral carbonation [41]. Furthermore, Koukouzas et al. [41], have calculated the CO_2 storage capacity (SC_{CO2}) using Equation (5).

$$SC_{CO_2}(\text{ton}) = \sum (V \times \varphi \times \rho \times \varepsilon) \quad (5)$$

The outcrop volume (V) of the Segamat basalt is 52 km^3 with an area of about 200 km^2 and a depth of 260 m. A potential plot with a volume of 0.0042 km^3 (length 400 m, width 250 m, depth 42 m) was used to estimate the CO_2 storage of the Segamat basalt outcrop. Also, the average porosity (φ) of the Segamat basalt samples is 16%. Studies in [42] and [43] have shown that the specific gravity of the carbon dioxide is 400 kg/m^3 at a pressure of 10 MPa and temperature of 50 °C. The CO_2 storage ratio (ε) is 5% [44]. Therefore, the Segamat basalt provides a site that could sequester 91,520 tons of carbon dioxide.

5. Conclusions

This study was undertaken in order to characterize samples of the Paleogene Segamat basalt in the Central Belt, Malaysia, to assess their potential in the process of CO_2 mineral carbonation. The findings from the petrographic and mineralogical studies indicate that Segamat basalt contains silicate minerals that are well favored in the process of CO_2 mineral carbonation. These are enstatite, augite, fayalite, and forsterite, which can form carbonate minerals (i.e., calcite, magnesite, and siderite) during reaction with CO_2. The results also show that the Segamat basalt samples have the necessary, appropriate physicochemical characteristics to be considered as potential sites for implementing the CO_2 mineral carbonation approach. Based on these characterizations, Segamat basalt might be considered as having the potential for mineral carbonation either for CO_2 storage purposes or ex situ mineral carbonation feedstock. Therefore, the Segamat basalt could be used in further studies to better understand the process of mineral carbonation in basalts.

Author Contributions: Conceptualization, S.A.A. and H.T.; methodology, O.R.; software S.A.A.; validation, writing—original draft preparation, S.A.A. and H.T.; writing—review and editing, O.R. and A.B.P.; supervision, H.T. and O.R. and A.B.P. All authors have read and agreed to the published version of the manuscript.

Funding: This project was funded by an industry research grant [0153CB–025] and University Research Internal Fund [0156LB0–046].

Acknowledgments: The authors would like to express their sincere gratitude to PETRONAS Research Sdn Bhd, and Universiti Teknologi PETRONAS (UTP) for the technical and financial support they received to carry out the research related to CO_2 mineral carbonation. Also, the Institute of Oceanography and Environment (INOS), Universiti Malaysia Terengganu (UMT) is acknowledged.

Conflicts of Interest: The authors declare no conflict of interest.

References

1. Bao, W.; Zhao, H.; Li, H.; Li, S.; Lin, W. Process simulation of mineral carbonation of phosphogypsum with ammonia under increased CO_2 pressure. *J. Co2 Util.* **2017**, *17*, 125–136. [CrossRef]
2. Rahmani, O. Siderite precipitation using by–product red gypsum for CO_2 sequestration. *J. Co2 Util.* **2018**, *24*, 321–327. [CrossRef]
3. Rahmani, O.; Junin, R.; Tyrer, M.; Mohsin, R. Mineral carbonation of red gypsum for CO_2 sequestration. *Energy Fuels* **2014**, *28*, 5953–5958. [CrossRef]
4. Rahmani, O. CO_2 sequestration by indirect mineral carbonation of industrial waste red gypsum. *J. Co2 Util.* **2018**, *27*, 374–380. [CrossRef]
5. Bachu, S.; Bonijoly, D.; Bradshaw, J.; Burruss, R.; Holloway, S.; Christensen, N.P.; Mathiassen, O.M. CO_2 storage capacity estimation: Methodology and gaps. *Int. J. Greenh. Gas Control* **2007**, *1*, 430–443. [CrossRef]
6. Rahman, F.A.; Aziz, M.M.A.; Saidur, R.; Bakar, W.A.W.A.; Hainin, M.; Putrajaya, R.; Hassan, N.A. Pollution to solution: Capture and sequestration of carbon dioxide (CO_2) and its utilization as a renewable energy source for a sustainable future. *Renew. Sustain. Energy Rev.* **2017**, *71*, 112–126. [CrossRef]
7. Depaolo, D.J.; Cole, D.R. Geochemistry of Geologic Carbon Sequestration: An Overview. *Rev. Miner. Geochem.* **2013**, *77*, 1–14. [CrossRef]
8. Jun, Y.-S.; Giammar, D.E.; Werth, C.J. Impacts of Geochemical Reactions on Geologic Carbon Sequestration. *Environ. Sci. Technol.* **2013**, *47*, 3–8. [CrossRef]
9. Rahmani, O.; Kadkhodaie, A.; Highfield, J. Kinetics analysis of CO_2 mineral carbonation using byproduct red gypsum. *Energy Fuels* **2016**, *30*, 7460–7464. [CrossRef]
10. Olajire, A.A. A review of mineral carbonation technology in sequestration of CO_2. *J. Pet. Sci. Eng.* **2013**, *109*, 364–392. [CrossRef]
11. Naraharisetti, P.K.; Yeo, T.Y.; Bu, J. New classification of CO_2 mineralization processes and economic evaluation. *Renew. Sustain. Energy Rev.* **2019**, *99*, 220–233. [CrossRef]
12. Rahmani, O. An experimental study of accelerated mineral carbonation of industrial waste red gypsum for CO_2 sequestration. *J. Co2 Util.* **2020**, *35*, 265–271. [CrossRef]
13. Dichicco, M.C.; Laurita, S.; Paternoster, M.; Rizzo, G.; Sinisi, R.; Mongelli, G. Serpentinite carbonation for CO_2 sequestration in the southern Apennines: Preliminary study. *Energy Procedia* **2015**, *76*, 477–486. [CrossRef]
14. Kelemen, P.B.; Matter, J.; Streit, E.E.; Rudge, J.F.; Curry, W.B.; Blusztajn, J. Rates and mechanisms of mineral carbonation in peridotite: Natural processes and recipes for enhanced, in situ CO_2 capture and storage. *Annu. Rev. Earth Planet. Sci.* **2011**, *39*, 545–576. [CrossRef]
15. Rahmani, O.; Highfield, J.; Junin, R.; Tyrer, M.; Pour, A.B. Experimental Investigation and Simplistic Geochemical Modeling of CO_2 Mineral Carbonation Using the Mount Tawai Peridotite. *Molecules* **2016**, *21*, 353. [CrossRef]
16. Sanna, A.; Gaubert, J.; Maroto–Valer, M.M. Alternative regeneration of chemicals employed in mineral carbonation towards technology cost reduction. *Chem. Eng. J.* **2016**, *306*, 1049–1057. [CrossRef]
17. Rahmani, O.; Tyrer, M.; Junin, R. Calcite precipitation from by–product red gypsum in aqueous carbonation process. *Rsc Adv.* **2014**, *4*, 45548–45557. [CrossRef]
18. Sanna, A.; Uibu, M.; Caramanna, G.; Kuusik, R.; Maroto–Valer, M.M. A review of mineral carbonation technologies to sequester CO_2. *Chem. Soc. Rev.* **2014**, *43*, 8049–8080. [CrossRef]
19. Oelkers, E.H.; Gislason, S.R.; Matter, J. Mineral carbonation of CO_2. *Elements* **2008**, *4*, 333–337. [CrossRef]
20. Matter, J.M.; Takahashi, T.; Goldberg, D. Experimental evaluation of in situ CO_2-water-rock reactions during CO_2 injection in basaltic rocks: Implications for geological CO_2 sequestration. *Geochem. Geophys. Geosyst.* **2007**, *8*, 1–19. [CrossRef]
21. McGrail, B.P.; Schaef, H.T.; Ho, A.M.; Chien, Y.J.; Dooley, J.J.; Davidson, C.L. Potential for carbon dioxide sequestration in flood basalts. *J. Geophys. Res. Solid Earth* **2006**, *111*, B12201. [CrossRef]

22. Gislason, S.R.; Wolff–Boenisch, D.; Stefansson, A.; Oelkers, E.H.; Gunnlaugsson, E.; Sigurdardottir, H.; Stute, M. Mineral sequestration of carbon dioxide in basalt: A pre–injection overview of the CarbFix project. *Int. J. Greenh. Gas Control* **2010**, *4*, 537–545. [CrossRef]
23. O'Connor, W.K.; Rush, G.E.; Dahlin, D.C. Laboratory Studies on the Carbonation Potential of Basalt; applications to geological sequestration of CO_2 in the Columbia River Basalt Group. In *AAPG Annual Meeting Expanded Abstracts*; American Association of Petroleum Geologists: Salt Lake City, UT, USA, 2003.
24. Callow, B.; Falcon–Suarez, I.; Ahmed, S.; Matter, J. Assessing the carbon sequestration potential of basalt using X–ray micro–CT and rock mechanics. *Int. J. Greenh. Gas Control* **2018**, *70*, 146–156. [CrossRef]
25. Metcalfe, I. Palaeozoic–Mesozoic history of SE Asia. *Geol. Soc. Lond. Spec. Publ.* **2011**, *355*, 7–35. [CrossRef]
26. Metcalfe, I. Tectonic framework and Phanerozoic evolution of Sundaland. *Gondwana Res.* **2011**, *19*, 3–21. [CrossRef]
27. Metcalfe, I. Tectonic evolution of the Malay Peninsula. *J. Asian Earth Sci.* **2013**, *76*, 195–213. [CrossRef]
28. Peng, L.C.; Leman, M.S.; Nasib, B.; Karim, R. *Stratigraphic Lexicon of Malaysia*; Geological Society of Malaysia: Kuala Lumpur, Malaysia, 2004.
29. Chakraborty, K.; Kaminen, D. *Chemical Characteristics and Classification of Segamat Volcanics*; Geological Society of Malaysia: Kuala Lumpur, Malaysia, 1978.
30. Grubb, P. Undersaturated potassic lavas and hypabyssal intrusives in north Johore. *Geol. Mag.* **1965**, *102*, 338–346. [CrossRef]
31. Hutchison, C.; Tan, D. *Geology of Peninsular Malaysia*; University of Malaya/Geological Society of Malaysia: Kuala Lumpur, Malaysia, 2009.
32. Bignell, J.; Snelling, N. K-Ar Ages on Some Basic Igneous Rocks from Peninsular Malaysia and Thailand. *Bull. Geol. Soc. Malays.* **1997**, *8*, 89–93. [CrossRef]
33. Abdullah, I.; Setiawan, J.; Awalnur, S. Sistem Sesar Dalam Basalt Segamat: Kaji. Kes Di Kuari Yam Fong (Malay). *Bull. Geol. Soc. Malays.* **1997**, *48*, 111–114. [CrossRef]
34. Ng, T.F.; Tate, R.B.; Tan, D.N.K. *Geological Map of Peninsular Malaysia*; Scale 1:1 000 000; Geological Society of Malaysia & University Malaya: Kuala Lumpur, Malaysia, 2008.
35. Jerram, D.; Petford, N. *The Field Description of Igneous Rocks*; John Wiley & Sons: Hoboken, NJ, USA, 2011.
36. Kalnicky, D.J.; Singhvi, R. Field portable XRF analysis of environmental samples. *J. Hazard. Mater.* **2001**, *83*, 93–122. [CrossRef]
37. Snellings, R.; Bazzoni, A.; Scrivener, K. The existence of amorphous phase in Portland cements: Physical factors affecting Rietveld quantitative phase analysis. *Cem. Concr. Res.* **2014**, *59*, 139–146. [CrossRef]
38. Kashim, M.Z.; Tsegab, H.; Rahmani, O.; Affendi, A.B.Z.; Aminpour, S.M. Reaction Mechanism of Wollastonite In Situ Mineral Carbonation for CO_2 Sequestration: Effects of Saline Conditions, Temperature, and Pressure. *ACS Omega* **2020**, *5*, 28942–28954. [CrossRef]
39. Dessert, C.; Dupré, B.; Gaillardet, J.; François, L.M.; Allegre, C.J. Basalt weathering laws and the impact of basalt weathering on the global carbon cycle. *Chem. Geol.* **2003**, *202*, 257–273. [CrossRef]
40. Gislason, S.R.; Broecker, W.S.; Gunnlaugsson, E.; Snæbjörnsdóttir, S.; Mesfin, K.G.; Alfredsson, H.A.; Aradottir, E.S.; Sigfusson, B.; Gunnarsson, I.; Stute, M.; et al. Rapid solubility and mineral storage of CO_2 in basalt. *Energy Procedia* **2014**, *63*, 4561–4574. [CrossRef]
41. Koukouzas, N.; Koutsovitis, P.; Tyrologou, P.; Karkalis, C.; Arvanitis, A. Potential for Mineral Carbonation of CO_2 in Pleistocene Basaltic Rocks in Volos Region (Central Greece). *Minerals* **2019**, *9*, 627. [CrossRef]
42. Span, R.; Wagner, W. A new equation of state for carbon dioxide covering the fluid region from the triple-point temperature to 1100 K at pressures up to 800 MPa. *J. Phys. Chem. Ref. Data* **1996**, *25*, 1509–1596. [CrossRef]
43. Spycher, N.; Pruess, K. CO_2-H_2O mixtures in the geological sequestration of CO_2. II. Partitioning in chloride brines at 12–100_C and up to 600 bar. *Geochim. Cosmochim. Acta* **2005**, *69*, 3309–3320. [CrossRef]
44. Gislason, S.; Oelkers, E. Carbon Storage in Basalt. *Science* **2014**, *344*, 373–374. [CrossRef]